

Optical properties of Er³⁺-doped tungsten tellurite glass waveguides by Ag⁺–Na⁺ ion-exchange

Shinichi Sakida ^{a,*}, Tokuro Nanba ^b, Yoshinari Miura ^b

^a Environmental Management and Safety Section, Health and Environment Center, Okayama University, 3-1-1, Tsushima-Naka, Okayama-shi 700-8530, Japan

^b Department of Environmental Chemistry and Materials, Faculty of Environmental Science and Technology, Okayama University, 3-1-1, Tsushima-Naka, Okayama-shi 700-8530, Japan

Received 19 October 2006; received in revised form 19 December 2006; accepted 18 January 2007

Available online 6 March 2007

Abstract

The planar waveguides of 12Na₂O · 35WO₃ · 53TeO₂ · 1Er₂O₃ glass (in mol%) were prepared by Ag⁺–Na⁺ ion-exchange at 300–360 °C for 5–30 h. The effective mode indices and propagation losses of the waveguides were measured at the wavelengths of 473, 632.8, 983.1 and 1548 nm by means of a prism coupler technique. The waveguide depths from glass surface increased with increasing ion-exchange temperature and time. The diffusion parameters such as diffusion coefficient and activation energy were calculated on the basis of an Arrhenius temperature dependence of the diffusion coefficient of Ag⁺ ions in the ion-exchanged glasses. The propagation losses of the waveguides were 5.04–6.64, 2.70–4.77, 5.44–6.73 and 7.32–8.31 dB/cm in the first half in the propagation distance from 0 to 3.0 cm and 3.52–4.82, 1.92–2.99, 3.78–5.06 and 3.91–5.15 dB/cm in the latter half at 473, 632.8, 983.1 and 1548 nm, respectively. The relationship between the optical properties of the waveguides and the ion-exchange conditions is discussed.

© 2007 Elsevier B.V. All rights reserved.

PACS: 42.70.Ce; 42.79.Gn

Keywords: Tellurite glass; Ion-exchange; Optical waveguides; Refractive-index profiles; Diffusion parameters; Propagation losses

1. Introduction

Since Er³⁺-doped tellurite glasses exhibit larger stimulated emission cross sections and broader emission bandwidth than Er³⁺-doped silica, silicate, phosphate and fluoride glasses at the 1.5 μm band [1–5], these glasses are the good candidates as 1.5 μm broadband amplifier host materials for development of wavelength division multiplexing (WDM) telecommunication system.

The planar waveguides compose the basis for integrated optical devices applicable to amplifiers and laser for high-speed signal processing in telecommunications. The planar waveguides allow the development of low-cost and com-

pact devices to be used in metropolitan and local access networks.

The fabrication of planar waveguides has been achieved by various techniques such as ion-exchange [6–14], sol–gel [15], plasma enhanced chemical vapor deposition (PECVD) [16], physical vapor deposition (PVD) [17], flame hydrolysis deposition (FHD) [18], pulsed laser deposition (PLD) [19,20], rf-sputtering [21,22] and laser writing [23,24]. Among these techniques, an ion-exchange method has been recognized as a powerful technique for waveguide fabrication in glass due to its simplicity, flexibility, effectiveness, reliability and low cost. So far, Ag⁺–Na⁺ and K⁺–Na⁺ ion-exchanges were carried out on silicate [8,9], soda-lime [10], borosilicate [11] and phosphate [12,13] glasses. However, only a few papers report the fabrication of waveguides in tungsten tellurite glasses by Ag⁺–Na⁺

* Corresponding author. Tel.: +81 86 251 7279; fax: +81 86 251 7281.
E-mail address: sakida@cc.okayama-u.ac.jp (S. Sakida).

ion-exchange [6,7,14] although the waveguide amplifier in a tellurite glass is expected to exhibit high optical gain and to be low-cost and compact. Therefore, the further information about the fabrication and characterization of tellurite glass waveguides by ion-exchange is required.

In the present study, the planar waveguides of an Er^{3+} -doped tungsten tellurite glass are prepared by Ag^+ – Na^+ ion-exchange under various conditions. The optical properties of the waveguides are characterized.

2. Experimental

2.1. Glass preparation and ion-exchange

2.1.1. Glass preparation

A tungsten tellurite glass with $12\text{Na}_2\text{O} \cdot 35\text{WO}_3 \cdot 53\text{TeO}_2 \cdot 1\text{Er}_2\text{O}_3$ composition in mol% was prepared as a substrate glass. In the preparation of the tellurite glass, high purity reagents of Na_2CO_3 , WO_3 , TeO_2 and Er_2O_3 were used as starting materials. The glass was prepared according to the following procedure: A 20 g batch of well-mixed reagents was melted in a gold crucible covered with a lid using an electric furnace at 800 °C for 30 min in air. The melt was poured onto a brass plate and immediately pressed by a stainless plate. The prepared glass was annealed near the glass-transition temperature for 1 h. After annealing, the glass was cut into a plate of $50 \times 15 \times 2$ mm in size and all faces mirror-polished for optical measurements and waveguide fabrication. Finally the glass was transparent and orange due to the small amount of erbium.

2.1.2. Ion-exchange

For waveguide fabrication, Ag^+ – Na^+ ion-exchange was performed by immersing the glass samples in $1.0\text{AgNO}_3 \cdot 49.5\text{NaNO}_3 \cdot 49.5\text{KNO}_3$ (mol%) molten salt at 300–360 °C for 5 h and at 360 °C for 10–30 h in air. The fresh molten salt was stirred and thermostated in a square alumina bath. The bath was stabilized within ± 1 °C from a nominal temperature, while the actual melt temperature was monitored by immersing a shielded thermocouple. Before ion-exchange, each sample was cleaned in distilled water and ethanol. All the samples were immersed below the glass-transition temperature (T_g) in order to prevent softening and crystallization. After ion-exchange, the samples were pulled out of the bath and slowly cooled to room temperature. Then the samples were washed with distilled water and ethanol to remove residuals of the bath and dried in air.

2.2. Measurement

2.2.1. Density measurement

The density of the substrate glass was measured by the Archimedes' method using kerosene as an immersion liquid at room temperature (21 °C). The experimental error was within $\pm 0.003 \text{ g cm}^{-3}$.

2.2.2. Thermal analyses

The glass-transition temperature (T_g) of the substrate glass was determined with a Rigaku Thermoflex TAS 300 TG 8110D TG-DTA. The measurement was carried out in air at a heating rate of $10 \text{ K} \cdot \text{min}^{-1}$. The experimental error in T_g was within ± 2 °C.

2.2.3. Refractive indices, effective mode indices and propagation losses

The refractive indices of the substrate glass and the effective mode indices and propagation losses of the waveguides at the wavelengths of 473, 632.8, 983.1 and 1548 nm were measured by means of a prism coupler technique (Metricron Model 2010 Prism Coupler).

3. Results

3.1. Substrate glass

Table 1 lists the density (ρ), glass-transition temperature (T_g), and refractive indices at wavelengths of 473, 632.8, 983.1 and 1548 nm (n_{473} , $n_{632.8}$, $n_{983.1}$ and n_{1548} , respectively) of $12\text{Na}_2\text{O} \cdot 35\text{WO}_3 \cdot 53\text{TeO}_2 \cdot 1\text{Er}_2\text{O}_3$ substrate glass. The density and T_g of the substrate glass were 5.896 g/cm^3 and 374.2 °C, respectively. The refractive indices of the glass were high (more than 2) and increased with decreasing wavelength.

3.2. Effective mode indices

Table 2 gives the number of modes and effective mode indices at wavelengths of 473, 632.8, 983.1, and 1548 nm for $12\text{Na}_2\text{O} \cdot 35\text{WO}_3 \cdot 53\text{TeO}_2 \cdot 1\text{Er}_2\text{O}_3$ glass ion-exchanged at 300–360 °C for 5 h and at 360 °C for 10–30 h. No mode at 1548 nm was observed for the waveguide fabricated by ion-exchange at 300 °C for 5 h. The number of modes of the waveguides fabricated by ion-exchange at 360 °C for 10–30 h was not able to be accurately counted at 473, 632.8 and 983.1 nm owing to very weak mode intensity. Since modes were observed for all the glasses ion-exchanged in this study, it can be said that we succeeded in fabricating the planar waveguides in the glass under all the ion-exchange conditions in this study. The effective mode indices obtained were higher than the refractive index of the substrate glass at the same wavelength. The number of modes increased with decreasing wavelength.

Table 1

Density (ρ), glass-transition temperature (T_g), and refractive indices at wavelengths of 473, 632.8, 983.1 and 1548 nm (n_{473} , $n_{632.8}$, $n_{983.1}$ and n_{1548} , respectively) of $12\text{Na}_2\text{O} \cdot 35\text{WO}_3 \cdot 53\text{TeO}_2 \cdot 1\text{Er}_2\text{O}_3$ substrate glass

$\rho/\text{g cm}^{-3}$	$T_g/^\circ\text{C}$	n_{473}	$n_{632.8}$	$n_{983.1}$	n_{1548}
5.896	374.2	2.1362	2.0720	2.0298	2.0103

The errors in ρ , T_g and n are within $\pm 0.003 \text{ g} \cdot \text{cm}^{-3}$, ± 2 °C and ± 0.001 , respectively.

Table 2
Ion-exchange conditions and the number of modes and effective mode indices at wavelengths of 473, 632.8, 983.1 and 1548 nm for ion-exchanged $12\text{Na}_2\text{O} \cdot 35\text{WO}_3 \cdot 53\text{TeO}_2 \cdot 1\text{Er}_2\text{O}_3$ glasses

Ion-exchange condition	Wavelength/nm	No. of modes	Effective mode index
300 °C, 5 h	473	2	2.1912, 2.1517
	632.8	2	2.1082, 2.0742
	983.1	1	2.0457
	1548	0 ^a	— ^a
310 °C, 5 h	473	3	2.2030, 2.1640, 2.1425
	632.8	2	2.1190, 2.0814
	983.1	1	2.0566
	1548	1	2.0195
320 °C, 5 h	473	4	2.2109, 2.1741, 2.1514, 2.1385
	632.8	3	2.1267, 2.0898, 2.0729
	983.1	2	2.0633, 2.0305
	1548	1	2.0270
330 °C, 5 h	473	5	2.2154, 2.1851, 2.1613, 2.1456, 2.1379
	632.8	3	2.1308, 2.0968, 2.0780
	983.1	2	2.0673, 2.0337
	1548	1	2.0309
340 °C, 5 h	473	6	2.2318, 2.2044, 2.1794, 2.1620, 2.1491, 2.1406
	632.8	4	2.1445, 2.1123, 2.0902, 2.0781
	983.1	3	2.0831, 2.0450, 2.0308
	1548	2	2.0464, 2.0111
350 °C, 5 h	473	8	2.2303, 2.2111, 2.1932, 2.1768, 2.1624, 2.1512, 2.1430, 2.1386
	632.8	5	2.1499, 2.1251, 2.1040, 2.0877, 2.0772
	983.1	3	2.0916, 2.0571, 2.0361
	1548	2	2.0568, 2.0171
360 °C, 5 h	473	11	2.2338, 2.2253, 2.2126, 2.2011, 2.1891, 2.1785, 2.1676, 2.1581, 2.1498, 2.1433, 2.1391
	632.8	8	2.1551, 2.1407, 2.1259, 2.1113, 2.0982, 2.0870, 2.0784, 2.0737
	983.1	5	2.1018, 2.0773, 2.0560, 2.0391, 2.0310
	1548	3	2.0709, 2.0348, 2.0133
360 °C, 10 h ^b	1548	4	2.0797, 2.0516, 2.0285, 2.0140
360 °C, 20 h ^b	1548	6	2.0866, 2.0714, 2.0534, 2.0368, 2.0230, 2.0138
360 °C, 30 h ^b	1548	7	2.0875, 2.0739, 2.0587, 2.0440, 2.0319, 2.0212, 2.0143

^a A mode at 1548 nm was not observed for the waveguide fabricated by ion-exchange at 300 °C for 5 h.

^b Modes at 473, 632.8 and 983.1 nm for the waveguides fabricated by ion-exchange at 360 °C for 10–30 h were not able to be accurately counted owing to very weak mode intensity.

The number of modes at the same wavelength increased with increasing ion-exchange temperature and time.

3.3. Propagation losses

The optical propagation loss curve of a $12\text{Na}_2\text{O} \cdot 35\text{WO}_3 \cdot 53\text{TeO}_2 \cdot 1\text{Er}_2\text{O}_3$ glass waveguide by ion-exchange

at 330 °C for 5 h at 632.8 nm is shown in Fig. 1. A propagation loss can be obtained by fitting an exponential curve to an experimental curve because a loss is defined by the next equation:

$$\text{Loss (dB)} = 10 \log_{10}(I_{\text{in}}/I_{\text{out}}) \quad (1)$$

where I_{in} and I_{out} are input and output intensities, respectively. The fitted loss curve is also plotted in the figure. The fitted curve agreed well with the experimental one in propagation distance from 0 to about 1.5 cm whereas the gaps between experimental and fitted curves began to appear at propagation distance of about 1.5 cm and increased with increasing propagation distance from 1.5 cm. Similarly, the fitted curves agreed well with the experimental loss curves for all the waveguides ion-exchanged in this study in the propagation distance from 0 to about 1.5 cm. Thus, it was difficult to exactly fit the exponential curves to the experimental loss curves of all the waveguides in this study in measured range of 0–3.0 cm. This effect indicates that the exponential attenuation does not follow the usual exponential behavior. The effective mode indices and propagation losses of the waveguides were measured under low coupling pressures (20–30 psi). The observed mode patterns of the waveguides had no distortion by overcoupling. The same effect was obtained for different coupling pressures. Hence, this effect is not owing to mode overcoupling. Since the same effect was observed for different directions of the propagating beam and different coupling points, the loss measurements are reproducible. The losses were measured in TE₀ configuration. Therefore, the loss measurements are reasonable. This effect is perhaps due to the gradual refractive-index change in ion-exchange layer although the definitive evidence to demonstrate the hypothesis has not been obtained yet. Since the gaps between experimental and fitted curves of the waveguides began to appear from the propagation distance of about

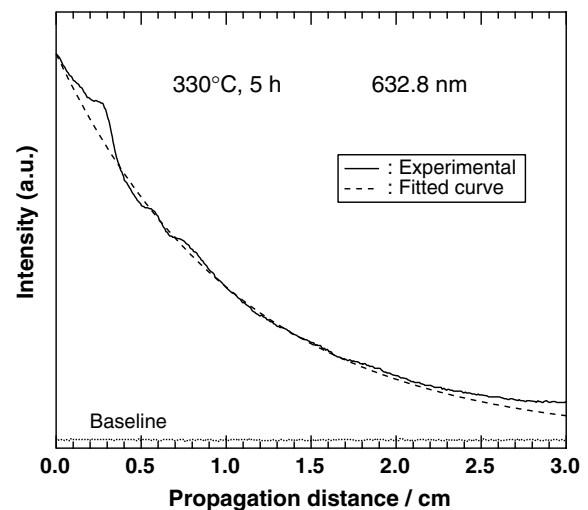


Fig. 1. Optical propagation loss curve of a $12\text{Na}_2\text{O} \cdot 35\text{WO}_3 \cdot 53\text{TeO}_2 \cdot 1\text{Er}_2\text{O}_3$ glass waveguide by ion-exchange at 330 °C for 5 h at 632.8 nm.

1.5 cm, we tried to obtain the propagation losses in two ranges of 0–1.5 and 1.5–3.0 cm on the assumption that the propagation loss changes at the propagation distance of about 1.5 cm. The trial enabled us to exactly fit the experimental curve in measured range of 0–3.0 cm using two exponential curves. The propagation losses (dB/cm) obtained by the fitting at wavelengths of 473, 632.8, 983.1, and 1548 nm for $12\text{Na}_2\text{O} \cdot 35\text{WO}_3 \cdot 53\text{TeO}_2 \cdot 1\text{Er}_2\text{O}_3$ glass waveguides are summarized in Table 3. Since a mode at 1548 nm for the waveguide ion-exchanged at 300 °C for 5 h was not observed, the loss data were not able to be obtained. The loss data of the waveguides ion-exchanged at 360 °C for 10–30 h were not able to be obtained at 473, 632.8, and 983.1 nm due to an indefinite first mode by very weak mode intensity.

Table 3
Propagation losses (dB/cm) at wavelengths of 473, 632.8, 983.1, and 1548 nm for $12\text{Na}_2\text{O} \cdot 35\text{WO}_3 \cdot 53\text{TeO}_2 \cdot 1\text{Er}_2\text{O}_3$ glass waveguides by various ion-exchange conditions

Ion-exchange condition	Propagation distance range	Propagation loss (dB/cm)			
		473 nm	632.8 nm	983.1nm	1548 nm
300 °C, 5 h	The first half ^a	5.04	2.70	5.44	— ^c
	The latter half ^b	3.52	2.18	3.78	— ^c
310 °C, 5 h	The first half ^a	5.30	2.95	6.17	7.82
	The latter half ^b	3.78	2.03	4.39	4.19
320 °C, 5 h	The first half ^a	5.99	3.52	5.93	7.35
	The latter half ^b	4.24	1.92	4.33	3.94
330 °C, 5 h	The first half ^a	6.46	3.99	6.67	7.90
	The latter half ^b	4.71	2.95	4.93	4.35
340 °C, 5 h	The first half ^a	6.16	4.77	6.73	8.31
	The latter half ^b	4.77	2.60	4.90	3.91
350 °C, 5 h	The first half ^a	6.32	3.79	6.49	7.90
	The latter half ^b	4.82	2.68	5.06	4.27
360 °C, 5 h	The first half ^a	6.64	4.25	6.68	7.85
	The latter half ^b	4.73	2.99	4.95	4.14
360 °C, 10 h	The first half ^a	— ^d	— ^d	— ^d	7.32
	The latter half ^b	— ^d	— ^d	— ^d	4.66
360 °C, 20 h	The first half ^a	— ^d	— ^d	— ^d	7.60
	The latter half ^b	— ^d	— ^d	— ^d	4.90
360 °C, 30 h	The first half ^a	— ^d	— ^d	— ^d	7.79
	The latter half ^b	— ^d	— ^d	— ^d	5.15

^a The first half = 0.0–about 1.5 cm.

^b The latter half = about 1.5–3.0 cm.

^c No loss data because a mode at 1548 nm was not observed.

^d No loss data due to an indefinite first mode by very weak mode intensity.

4. Discussion

4.1. Refractive-index profile

Fig. 2 shows refractive-index profiles at 632.8 nm for $12\text{Na}_2\text{O} \cdot 35\text{WO}_3 \cdot 53\text{TeO}_2 \cdot 1\text{Er}_2\text{O}_3$ glass waveguides by ion-exchange at 320–360 °C for 5 h. The horizontal broken line in the figure exhibits the glass substrate index. These profiles were obtained from the measured mode indices using an inverse Wentzel–Kramers–Brillouin (WKB) method [25] without assuming any particular shape. This method is applicable when at least three modes are observed. And its reliability increases with the increase in the number of the modes. The waveguide depths from glass surface increased with increasing ion-exchange temperature. The depths of the waveguides varied from about 3–7 μm with the increase in ion-exchange temperature. The glass surface refractive indices n_{surf} obtained by the refractive-index profiles were 2.1652–2.1767. Refractive-index changes from the glass substrate index were +0.0932 – +0.1047 for the waveguides, and very high. The refractive-index changes gave the similar values in spite of different ion-exchange temperatures and waveguide depths. This indicates that n_{surf} and refractive-index change are independent of the ion-exchange temperature and waveguide depth.

Fig. 3 shows refractive-index profiles at 1548 nm for $12\text{Na}_2\text{O} \cdot 35\text{WO}_3 \cdot 53\text{TeO}_2 \cdot 1\text{Er}_2\text{O}_3$ glass waveguides by ion-exchange at 360 °C for 5–30 h. The waveguide depths from glass surface increased with increasing ion-exchange time. The depths of the waveguides varied from about 7–15 μm with the increase in ion-exchange time. The n_{surf} of the waveguides were 2.0935–2.1076. Refractive-index changes from the glass substrate index were +0.0832–+0.0973 for the waveguides, and very high. The refractive-index changes gave the similar values in spite of different ion-exchange times and waveguide depths. This

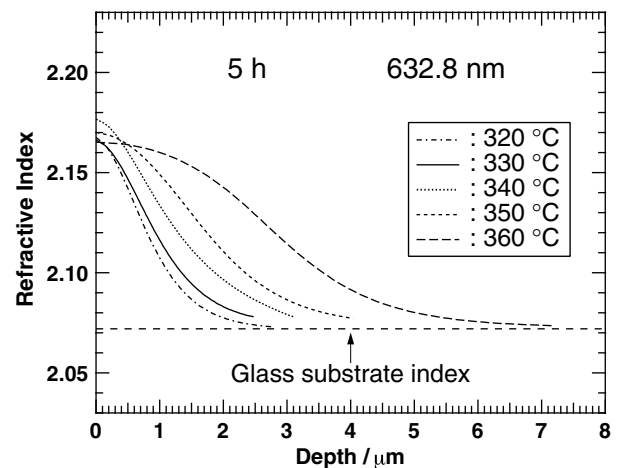


Fig. 2. Refractive-index profiles at 632.8 nm for $12\text{Na}_2\text{O} \cdot 35\text{WO}_3 \cdot 53\text{TeO}_2 \cdot 1\text{Er}_2\text{O}_3$ glass waveguides by ion-exchange at 320–360 °C for 5 h.

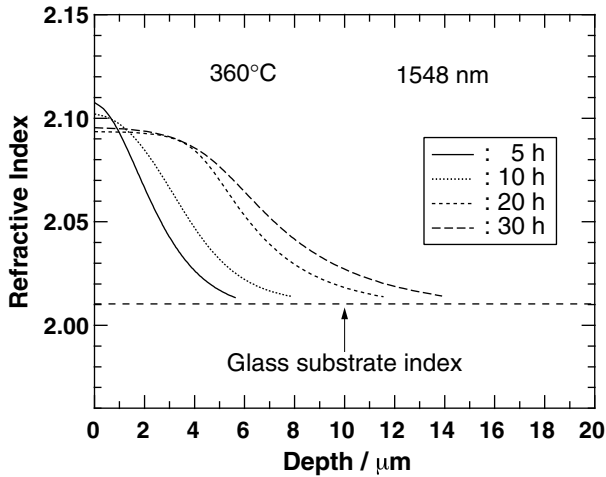


Fig. 3. Refractive-index profiles at 1548 nm for $12\text{Na}_2\text{O} \cdot 35\text{WO}_3 \cdot 53\text{TeO}_2 \cdot 1\text{Er}_2\text{O}_3$ glass waveguides by ion-exchange at 360°C for 5–30 h.

indicates that n_{surf} and refractive-index change are independent of the ion-exchange time and waveguide depth.

As seen in Figs. 2 and 3, the refractive indices of the waveguides were highest on the surfaces and decreased with increasing waveguide depth, corresponding the decrease of concentration of Ag^+ ions with the increase of waveguide depth.

4.2. Diffusion parameters

Refractive-index profiles can be fitted using Gaussian function [25] and expressed as follows [6]:

$$\begin{aligned} n(x) &= n_{\text{sub}} + (n_{\text{surf}} - n_{\text{sub}}) \exp(-x^2/d^2) \\ &= n_{\text{sub}} + \Delta n \exp(-x^2/d^2) \end{aligned} \quad (2)$$

where x is the depth from the surface of glass substrate, n_{sub} is the refractive index of glass substrate, n_{surf} is the refractive index of glass surface, Δn is the maximum index change at the surface ($x=0$) of the substrate, and d is the effective depth of the waveguide. When $x=d$, $n(d) = n_{\text{sub}} + \Delta n/e$. d is used as a representative depth to calculate the diffusion parameters of Ag^+ ions in the waveguide since the gradual refractive-index change of the waveguide with the depth make the determination of waveguide depth difficult.

d can be given by the following equation because of the diffusion process:

$$d = (D_e t)^{1/2} \quad (3)$$

where D_e is an effective diffusion coefficient, and t is the diffusion time, namely, ion-exchange time. The diffusion coefficient has Arrhenius temperature dependence:

$$D_e = D_0 \exp(-E_D/RT) \quad (4)$$

where D_0 is a pre-exponential factor, E_D is activation energy, T is the temperature in K unit, and R is the gas constant (8.314 J/Kmol). A d value can be obtained from a

measured refractive-index profile and Eq. (2), and D_e , D_0 and E_D values can be calculated on the basis of measured index profiles for various ion-exchange temperatures and times, and Eqs. (2)–(4).

The relationship between $\ln D_e$ at 632.8 nm and $1/T$ for $12\text{Na}_2\text{O} \cdot 35\text{WO}_3 \cdot 53\text{TeO}_2 \cdot 1\text{Er}_2\text{O}_3$ glass waveguides by ion-exchange at 320 – 360°C for 5 h is exhibited in Fig. 4. Here D_e was calculated based on refractive index profiles at 632.8 nm. Eq. (4) can be expressed as follows:

$$\ln D_e = \ln D_0 + (-E_D/R) \times (1/T) \quad (5)$$

where $\ln D_0$ and $(-E_D/R)$ mean an intercept and slope, respectively, of a straight line in the plot of $\ln D_e$ versus $(1/T)$. The experimental points in the figure were well fitted by the straight line illustrated in the figure. Therefore, it can be said that the diffusion of Ag^+ ions in the waveguides obeys Arrhenius temperature dependence. From the linear fit, we estimated $D_0 = 5.71 \times 10^3 \text{ cm}^2/\text{s}$ and $E_D = 182.65 \text{ kJ/mol}$ for the waveguides.

The d values of $12\text{Na}_2\text{O} \cdot 35\text{WO}_3 \cdot 53\text{TeO}_2 \cdot 1\text{Er}_2\text{O}_3$ glass waveguides are listed in Table 4. Here they were estimated from the refractive-index profiles at 632.8 and 1548 nm for the waveguides by ion-exchange at 320 – 360°C for 5 h and at 360°C for 5–30 h as seen in Figs. 2 and 3, respectively. The d values at 300 and 310°C for 5 h were calculated from the fitted straight line in Fig. 4 and Eq. (3). The d value at 360°C for 5 h at 632.8 nm ($3.30 \mu\text{m}$) is different from that at 1548 nm ($2.83 \mu\text{m}$).

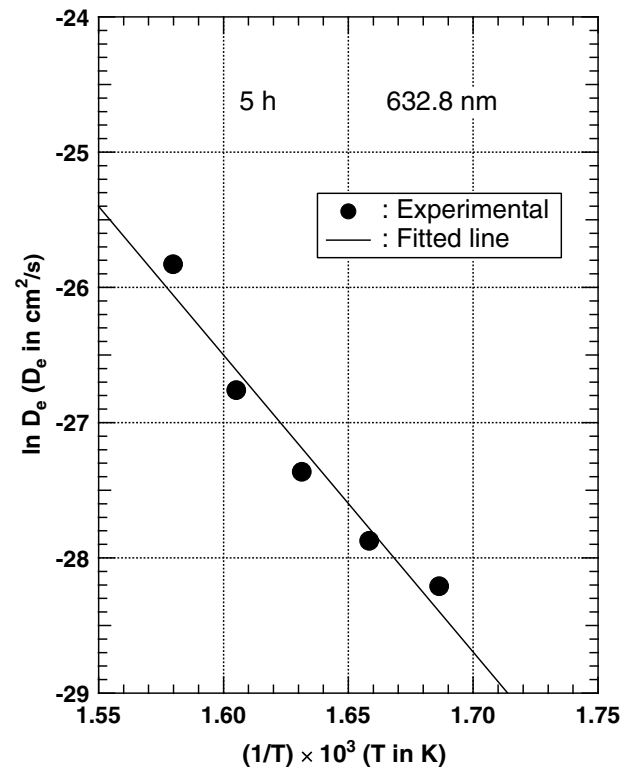


Fig. 4. Relationship between $\ln D_e$ at 632.8 nm and $1/T$ for $12\text{Na}_2\text{O} \cdot 35\text{WO}_3 \cdot 53\text{TeO}_2 \cdot 1\text{Er}_2\text{O}_3$ glass waveguides by ion-exchange at 320 – 360°C for 5 h.

Table 4

Effective depths (d) of $12\text{Na}_2\text{O} \cdot 35\text{WO}_3 \cdot 53\text{TeO}_2 \cdot 1\text{Er}_2\text{O}_3$ glass waveguides by various ion-exchange conditions. The d values at 300–360 °C for 5 h and at 360 °C for 5–30 h were obtained from the measurements at 632.8 and 1548 nm, respectively

Ion-exchange condition	$d/\mu\text{m}$	Wavelength/nm
300 °C, 5 h	0.48 ^a	632.8
310 °C, 5 h	0.67 ^a	632.8
320 °C, 5 h	1.01	632.8
330 °C, 5 h	1.19	632.8
340 °C, 5 h	1.53	632.8
350 °C, 5 h	2.08	632.8
360 °C, 5 h	3.30	632.8
360 °C, 5 h	2.83	1548
360 °C, 10 h	4.17	1548
360 °C, 20 h	6.86	1548
360 °C, 30 h	8.00	1548

^a The d values at 300 and 310 °C for 5 h were calculated from the fitted straight line in Fig. 4 and Eq. (3).

Taking into account the d value calculated from the fitted straight line in Fig. 4 at 360 °C for 5 h (2.95 μm), it can be said that the d value at 1548 nm is more reliable than that at 632.8 nm. Hence, the d value at 360 °C for 5 h at 1548 nm (2.83 μm) is used as that at 360 °C for 5 h hereafter. The d value monotonously increased with increasing ion-exchange temperature and time. The d value increased quickly with increasing ion-exchange temperature whereas it increased slowly with increasing ion-exchange time.

The relationship between effective depth d at 1548 nm and ion-exchange time t for $12\text{Na}_2\text{O} \cdot 35\text{WO}_3 \cdot 53\text{TeO}_2 \cdot 1\text{Er}_2\text{O}_3$ glass waveguides by ion-exchange at 360 °C for 5–30 h is illustrated in Fig. 5. The theoretical fitted curve for the diffusion is also shown. Since it fits the experimental points very well, the d of these waveguides obey the rule in Eq. (3) very well, indicating that the behavior of Ag^+ ions by the ion-exchange obeys the diffusion process. The D_e value at 360 °C and 1548 nm estimated from the fitting curve was $5.81 \times 10^{-4} \mu\text{m}^2/\text{s}$.

4.3. Propagation losses

As reported in Table 3, in the first half in propagation distance from 0 to 3.0 cm, the propagation losses were 5.04–6.64, 2.70–4.77, 5.44–6.73 and 7.32–8.31 dB/cm at 473, 632.8, 983.1 and 1548 nm, respectively. In the latter half the propagation losses were 3.52–4.82, 1.92–2.99, 3.78–5.06 and 3.91–5.15 dB/cm at 473, 632.8, 983.1 and 1548 nm, respectively. As a result, the magnitude of the losses in this study was the order of 1548 nm > 983.1 nm > 473 nm > 632.8 nm. The large losses at 983.1 and 1548 nm are due to the absorption of Er^{3+} ions [14]. The propagation losses in the latter half were smaller than those in the first half for all the ion-exchange conditions and wavelengths in this study. This result indicates that the propagation loss does not maintain a constant value but decreases with light attenuation in the waveguide. The losses of waveguide by ion-exchange at 300 °C for 5 h were the smallest

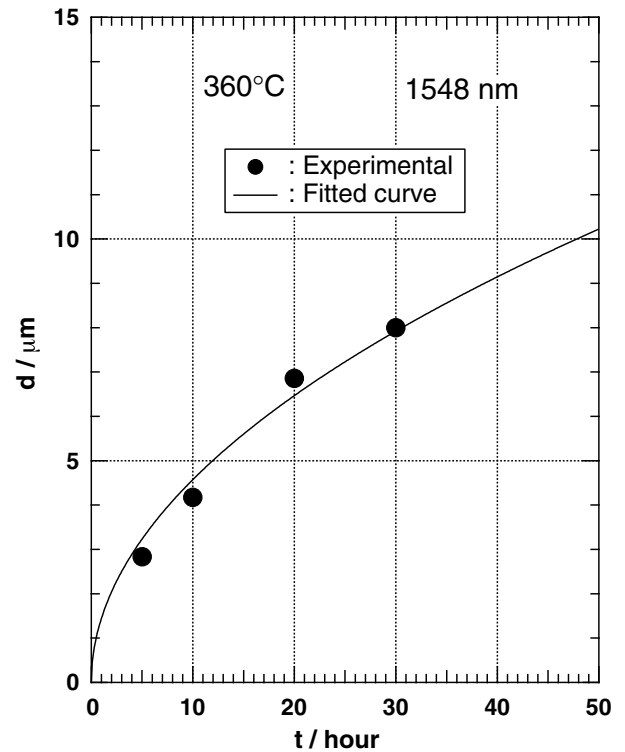


Fig. 5. Relationship between effective depth d at 1548 nm and ion-exchange time t for $12\text{Na}_2\text{O} \cdot 35\text{WO}_3 \cdot 53\text{TeO}_2 \cdot 1\text{Er}_2\text{O}_3$ glass waveguides by ion-exchange at 360 °C for 5–30 h.

except that at 632.8 nm in the latter half and those at 300–320 °C for 5 h at 473, 632.8 and 983.1 nm were slightly smaller than those at 330–360 °C for 5 h. On the other hand, the losses at 1548 nm in the first half were independent of ion-exchange temperature and time. In the latter half they were independent of ion-exchange temperature but slightly increased with increasing ion-exchange time. However, since the difference between maximum and minimum losses at each wavelength in the same propagation distance range was within about 2 dB/cm, it can be said that the propagation losses in this study are not very dependent on ion-exchange conditions as a whole.

Fig. 6 shows the relationship between propagation losses at wavelengths of 473, 632.8 and 983.1 nm (a) and 1548 nm (b) and effective depths d for $12\text{Na}_2\text{O} \cdot 35\text{WO}_3 \cdot 53\text{TeO}_2 \cdot 1\text{Er}_2\text{O}_3$ glass waveguides. The data about waveguides ion-exchanged at 300–360 °C for 5–30 h are plotted in the figure. The d values at 473, 632.8 and 983.1 nm are between 0.48 and 2.83 μm (Fig. 6a). Those at 1548 nm are between 0.67 and 8.00 μm (Fig. 6b). The losses with d more than 1 μm are slightly larger than those with d less than 1 μm at 473, 632.8 and 983.1 nm. The loss at 1548 nm in the latter half slightly increased with increasing d in the range of 2.83–8.00 μm . As a whole, however, the propagation losses in this study are not very dependent on the depths of the waveguides.

The tellurite waveguide by the pulsed laser deposition (PLD) of thin film of tellurite glasses doped with erbium

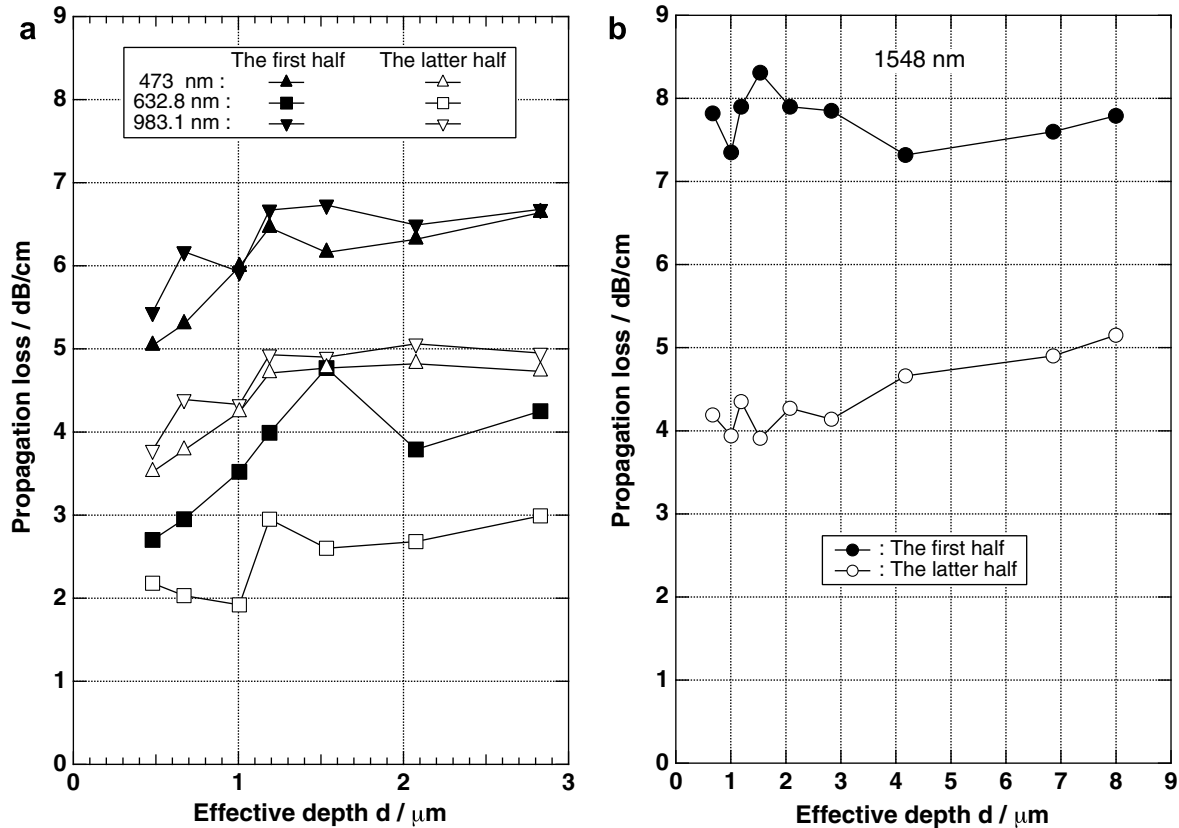


Fig. 6. Relationship between propagation losses at wavelengths of 473, 632.8 and 983.1 nm (a) and 1548 nm (b) and effective depths d for $12\text{Na}_2\text{O} \cdot 35\text{WO}_3 \cdot 53\text{TeO}_2 \cdot 1\text{Er}_2\text{O}_3$ glass waveguides.

ions presented a very high value of optical loss (approx. 20 ± 3 dB/cm) at 632 nm [19]. The optical losses of erbium-doped zinc-tellurite ($\text{TeO}_2\text{-ZnCl}_2\text{-ZnO}$) oxyhalide glass waveguides, deposited by reactive pulsed laser deposition (RPLD) on silica substrates were 0.8–11.5 dB/cm at 633 nm [20]. The optical losses of amorphous TeO_{2-x} films deposited on Corning glass substrates by reactive sputtering under different $\text{O}_2\text{:Ar}$ gas mixtures were 0.26–4.20 dB/cm at 633 nm [21]. Since the optical losses of the tellurite glass waveguides by $\text{Ag}^+\text{-Na}^+$ ion-exchange in the present study are 2.70–4.77 dB/cm (the first half) at 632.8 nm, they are relative small compared with losses of the tellurite waveguides by other methods as described above [19–21]. Hence, the tellurite glass waveguides fabricated by $\text{Ag}^+\text{-Na}^+$ ion-exchange are considered to be promising. Further work is needed to acquire lower optical losses of tellurite glass waveguides by $\text{Ag}^+\text{-Na}^+$ ion-exchange.

5. Conclusion

The planar waveguides of $12\text{Na}_2\text{O} \cdot 35\text{WO}_3 \cdot 53\text{-TeO}_2 \cdot 1\text{Er}_2\text{O}_3$ glass in mol% were fabricated by $\text{Ag}^+\text{-Na}^+$ ion-exchange under various conditions. The optical properties of these waveguides were characterized. The following conclusions were obtained.

- (1) The planar waveguides of the glass have been able to be fabricated by $\text{Ag}^+\text{-Na}^+$ ion-exchange at 300–360 °C for 5–30 h.
- (2) The refractive indices of the waveguides were highest on the surfaces and decreased with increasing waveguide depth. The glass surface refractive indices n_{surf} of the waveguides were about 0.1 larger than the glass substrate index. The n_{surf} gave the similar values in spite of different ion-exchange conditions and waveguide depths.
- (3) The effective depth of the waveguides from glass surface increased quickly with increasing ion-exchange temperature whereas it increased slowly with increasing ion-exchange time.
- (4) The diffusion of Ag^+ ions in the waveguides obeyed Arrhenius temperature dependence. The pre-exponential factor D_0 and activation energy E_D were $D_0 = 5.71 \times 10^3$ cm²/s and $E_D = 182.65$ kJ/mol for the waveguides.
- (5) The propagation losses of the waveguides were 5.04–6.64, 2.70–4.77, 5.44–6.73 and 7.32–8.31 dB/cm in the first half in propagation distance from 0 to 3.0 cm and 3.52–4.82, 1.92–2.99, 3.78–5.06 and 3.91–5.15 dB/cm in the latter half at 473, 632.8, 983.1 and 1548 nm, respectively. The magnitude of the propagation losses was the order of $1548 \text{ nm} > 983.1 \text{ nm} >$

473 nm > 632.8 nm. The propagation losses in the latter half were smaller than those in the first half.

- (6) The difference between maximum and minimum propagation losses at each wavelength in the same propagation distance range was within about 2 dB/cm. Therefore, the propagation losses are not very dependent on ion-exchange conditions and the depths of the waveguides as a whole.

References

- [1] Y. Ding, S. Jiang, B. Hwang, T. Luo, N. Peyghambarian, Y. Himei, T. Ito, Y. Miura, *Opt. Mater.* 15 (2000) 123.
- [2] S. Shen, M. Naftaly, A. Jha, *Opt. Commun.* 205 (2002) 101.
- [3] A. Jha, S. Shen, M. Naftaly, *Phys. Rev. B* 62 (2000) 6215.
- [4] L.L. Neindre, S. Jiang, B. Hwang, T. Luo, J. Watson, N. Peyghambarian, *J. Non-Cryst. Solids* 255 (1999) 97.
- [5] Y. Ohishi, A. Mori, M. Yamada, H. Ono, Y. Nishida, K. Oikawa, *Opt. Lett.* 23 (1998) 274.
- [6] Y. Ding, S. Jiang, T. Luo, Y. Hu, N. Peyghambarian, *Proc. SPIE-Int. Soc. Opt. Eng. (USA)* 4282 (2001) 23.
- [7] G.N. Conti, S. Berneschi, M. Bettinelli, M. Brenci, B. Chen, S. Pelli, A. Speghini, G.C. Righini, *J. Non-Cryst. Solids* 345&346 (2004) 343.
- [8] G.C. Righini, S. Pelli, M. Brenci, M. Ferrari, C. Duverger, M. Montagna, R. Dall'Igna, *J. Non-Cryst. Solids* 284 (2001) 223.
- [9] T. Yano, T. Nagano, J. Lee, S. Shibata, M. Yamane, *J. Non-Cryst. Solids* 270 (2000) 163.
- [10] C. De Bernardi, S. Morasca, D. Scarano, A. Carnera, M. Morra, *J. Non-Cryst. Solids* 119 (1990) 195.
- [11] T. Ohtsuki, S. Honkanen, N. Peyghambarian, M. Takahashi, Y. Kawamoto, J. Inghoff, A. Tervonen, K. Kadono, *Appl. Phys. Lett.* 69 (1996) 2012.
- [12] G. Sorbello, S. Taccheo, M. Marano, M. Marangoni, R. Osellame, R. Ramponi, P. Laporta, *Opt. Mater.* 17 (2001) 425.
- [13] E.V. Kolobkova, A.A. Lipovskii, C. Montero, J. Liñares, *J. Phys. D: Appl. Phys.* 32 (1999) L9.
- [14] S. Sakida, T. Nanba, Y. Miura, *Mater. Lett.* 60 (2006) 3413.
- [15] X. Orignac, D. Barbier, X.M. Du, R.M. Almeida, O. McCarthy, E. Yeatman, *Opt. Mater.* 12 (1999) 1.
- [16] J.W. Lee, S.S. Kim, B. Lee, J.H. Moon, *Appl. Surf. Sci.* 228 (2004) 271.
- [17] M.C. Marco de Lucas, C. Garapon, B. Jacquier, J. Mugnier, O. Frezza, O. Perrot, B. Boulard, C. Jacoboni, *Opt. Mater.* 10 (1998) 19.
- [18] K. Hattori, T. Kitagawa, M. Oguma, H. Okazaki, Y. Ohmori, *J. Appl. Phys.* 80 (1996) 5301.
- [19] M. Martino, A.P. Caricato, M. Fernández, G. Leggieri, A. Jha, M. Ferrari, M. Mattarelli, *Thin Solid Films* 433 (2003) 39.
- [20] A.P. Caricato, M. Fernández, M. Ferrari, G. Leggieri, M. Martino, M. Mattarelli, M. Montagna, V. Resta, L. Zampedri, R.M. Almeida, M.C. Gonçalves, L. Fortes, L.F. Santos, *Mater. Sci. Eng. B* 105 (2003) 65.
- [21] R. Nayak, V. Grpta, A.L. Dawar, K. Sreenivas, *Thin Solid Films* 445 (2003) 118.
- [22] A. Chiasera, C. Tosello, E. Moser, M. Montagna, R. Belli, R.R. Gonçalves, G.C. Righini, S. Pelli, A. Chiappini, L. Zampedri, M. Ferrari, *J. Non-Cryst. Solids* 322 (2003) 289.
- [23] Y. Tokuda, M. Saito, M. Takahashi, K. Yamada, W. Watanabe, K. Itoh, T. Yoko, *J. Non-Cryst. Solids* 326&327 (2003) 472.
- [24] A. Favre, E. Lee, V. Apostolopoulos, C.B.E. Gawith, C. Tai, E. Taylor, Y. Kondo, F. Koizumi, *Opt. Mater.* 27 (2004) 7.
- [25] K.S. Chiang, *J. Lightwave Technol.* LT-3 (1985) 385.